MECHANICAL ANALOGY FOR THE WAVE-PARTICLE: HELIX ON A VORTEX FILAMENT

VALERY P. DMITRIYEV

Received 22 October 2001 and in revised form 13 February 2002

The small amplitude-to-thread ratio helical configuration of a vortex filament in the ideal fluid behaves exactly as de Broglie wave. The complex-valued algebra of quantum mechanics finds a simple mechanical interpretation in terms of differential geometry of the space curve. The wave function takes the meaning of the velocity, with which the helix rotates about the screw axis. The helices differ in type of the screw—right- or left-handed. Two kinds of the helical waves deflect in the inhomogeneous fluid vorticity field in the same way as spin particles in the Stern-Gerlach experiment.

1. Introduction

In this paper, an earlier suggested [2] mechanical analog for quantum particles is further developed. A helical wave on a vortex filament in the ideal fluid is considered. It is shown to obey the linear Schrödinger equation. Other properties of a vortex filament also reproduce the specific features of a quantum object.

This work is a constituent of the whole project aimed at constructing a regular mechanical analogy of physical fields and particles. The approach is based on the concept of a substratum for physics. The substratum is a universal medium serving to model the waves and action-at-a-distance in vacuum. This medium is viewed mesoscopically as a turbulent ideal fluid. Perturbations of the turbulence model physical fields. In this way, equations that reproduce exactly the Maxwell's electromagnetic equations were derived [7]. The voids in the fluid give rise to dilatational inclusions, which serve as a model [3, 4] of charged particles.

Copyright © 2002 Hindawi Publishing Corporation
Journal of Applied Mathematics 2:5 (2002) 241–263
2000 Mathematics Subject Classification: 81P99, 76B47, 76B25, 35Q55, 37K40
URL: http://dx.doi.org/10.1155/S1110757X02110199

Microscopically the turbulent substratum is seen as a vortex sponge. The latter is postulated as an ideal fluid pierced in all directions by straight vortex tubes [6]. The hollow vortex tubes will be treated further as vortex filaments. We will consider a one-dimensional model of the vortex sponge with some recourse to higher dimensions. The microscopic construction presented here agrees well with respective mesoscopic models.

2. Vortex filament

The motion of an isolated vortex filament is governed by a dependence of the velocity $\mathbf{u}$ of the vortex filament's liquid element on the local form of the curve. To express such a law analytically, we need to describe the vortex filament as a space curve in the usual Frenet-Serret frame.

First, a point on a spatial curve is defined by the position vector $\mathbf{r}$, which is a function $\mathbf{r}(l)$ of the length l measured from a fiducial point along the curve. For a moving curve, there is a further dependence $\mathbf{r}(l,t)$ on the time t. Excluding information about the curve's space position, the local form of the curve is fully specified by its curvature $\kappa(l,t)$ and torsion $\tau(l,t)$. The latter are defined through the two unit vectors, a tangent

$$\mathbf{e}(l,t) = \frac{\partial \mathbf{r}}{\partial l} \tag{2.1}$$

and principal normal

$$\mathbf{n}(l,t) \tag{2.2}$$

(see Figure 2.1), by the Frenet-Serret formulae

$$\kappa \mathbf{n} = \frac{\partial \mathbf{e}}{\partial l}, \tag{2.3}$$

$$\tau \mathbf{n} = -\frac{\partial (\mathbf{e} \times \mathbf{n})}{\partial l}, \tag{2.4}$$

$$|\mathbf{e}| = 1, \qquad |\mathbf{n}| = 1. \tag{2.5}$$

The motion of the vortex filament without stretching is described in these terms by the Arms' equation

$$\mathbf{u}(l,t) = \frac{\partial \mathbf{r}}{\partial t} = \nu \kappa \mathbf{e} \times \mathbf{n}, \tag{2.6}$$

where ν stands for the coefficient of local self-induction and $\mathbf{e}$ is assumed to be parallel to the filament's vorticity vector (Figure 2.1; for a rigorous derivation see [1]). Using (2.1) and (2.3), (2.6) can be rewritten in the

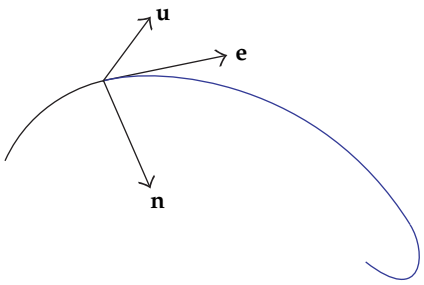

FIGURE 2.1. The drift **u** of a bent vortex filament in relation to its curvature $\kappa\mathbf{n}$ and vorticity **e**.

straightforward form

$$\frac{\partial \mathbf{r}}{\partial t} = \nu \frac{\partial \mathbf{r}}{\partial l} \times \frac{\partial^2 \mathbf{r}}{\partial l^2}. \tag{2.7}$$

3. Small disturbances

Let the filament be directed along the x-axis. We seek a solution to (2.7) in the form $\mathbf{r}(x,t)$ as small disturbances of the rectilinear configuration. This implies that

$$\left|\frac{\partial y}{\partial x}\right|, \left|\frac{\partial z}{\partial x}\right|, \left|\frac{\partial^2 y}{\partial x^2}\right|, \left|\frac{\partial^2 z}{\partial x^2}\right| \ll 1. \tag{3.1}$$

On this account, the corresponding quadratic terms is neglected throughout. So, we have for the arc's element

$$dl = \left[1 + \left(\frac{\partial y}{\partial x}\right)^2 + \left(\frac{\partial z}{\partial x}\right)^2\right]^{1/2} dx \approx dx, \tag{3.2}$$

and (2.7) can be rewritten as

$$\frac{\partial \mathbf{r}}{\partial t} = \nu \frac{\partial \mathbf{r}}{\partial x} \times \frac{\partial^2 \mathbf{r}}{\partial x^2}. \tag{3.3}$$

We have

$$\begin{aligned} \mathbf{r}(x,t) &= x\mathbf{i}_1 + y(x,t)\mathbf{i}_2 + z(x,t)\mathbf{i}_3, \\ \frac{\partial \mathbf{r}}{\partial x} &= \mathbf{i}_1 + \frac{\partial y}{\partial x}\mathbf{i}_2 + \frac{\partial z}{\partial x}\mathbf{i}_3, \\ \frac{\partial^2 \mathbf{r}}{\partial x^2} &= \frac{\partial^2 y}{\partial x^2}\mathbf{i}_2 + \frac{\partial^2 z}{\partial x^2}\mathbf{i}_3. \end{aligned} \tag{3.4}$$

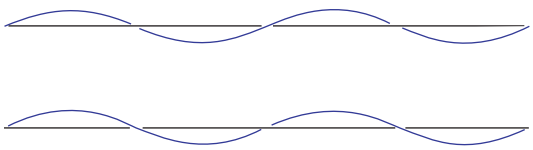

FIGURE 4.1. The right-hand screw helix (bottom) and the left-hand screw helix (top) in relation to the x-axis. The xz projection of (4.1) or (13.1) is shown.

This gives, for (3.3),

$$\frac{\partial \mathbf{r}}{\partial t} = v\mathbf{i}_1 \times \left(\frac{\partial^2 y}{\partial x^2}\mathbf{i}_2 + \frac{\partial^2 z}{\partial x^2}\mathbf{i}_3 \right). \tag{3.5}$$

Insofar as

$$\mathbf{i}_1 \times \left(y\mathbf{i}_2 + z\mathbf{i}_3 \right) = -z\mathbf{i}_2 + y\mathbf{i}_3, \tag{3.6}$$

the right-hand side of (3.5) does not contain the $\mathbf{i}_1$ component. This enables us to drop the respective term in the left-hand side

$$\frac{\partial y}{\partial t}\mathbf{i}_2 + \frac{\partial z}{\partial t}\mathbf{i}_3 = v\mathbf{i}_1 \times \left(\frac{\partial^2 y}{\partial x^2}\mathbf{i}_2 + \frac{\partial^2 z}{\partial x^2}\mathbf{i}_3 \right). \tag{3.7}$$

The latter form is convenient for further applications. So, it can be taken as the basic equation for small disturbances of the vortex filament in the ideal fluid.

The simplest shape for the initial configuration of the filament is given by a curve with constant curvature κ and torsion τ. In Sections 4 and 5, it is treated in two representations, which are equivalent to each other. First, we discuss it in vector form as implied by (3.7).

4. Vector mechanics

We consider a right-hand screw helix positioned along the x-axis

$$y = a\cos\left(\frac{x}{b}\right), \qquad z = a\sin\left(\frac{x}{b}\right), \tag{4.1}$$

where $a > 0$ is the amplitude and $b > 0$ the thread (or pitch) of the helix (Figure 4.1). This curve can be suggested as a small perturbation of the straight line if we take

$$a \ll b. \tag{4.2}$$

This gives for (2.1), (2.3), and (2.4), neglecting the small quantity a^2/b^2,

$$\mathbf{r} = x\mathbf{i}_1 + a\cos\left(\frac{x}{b}\right)\mathbf{i}_2 + a\sin\left(\frac{x}{b}\right)\mathbf{i}_3,$$

$$dl = |dr| = \left(1 + \frac{a^2}{b^2}\right)^{1/2} dx \approx dx, \tag{4.3}$$

$$\mathbf{e} = \mathbf{i}_1 + \frac{a}{b}\left[-\sin\left(\frac{x}{b}\right)\mathbf{i}_2 + \cos\left(\frac{x}{b}\right)\mathbf{i}_3\right],$$

$$\kappa\mathbf{n} = -\frac{a}{b^2}\left[\cos\left(\frac{x}{b}\right)\mathbf{i}_2 + \sin\left(\frac{x}{b}\right)\mathbf{i}_3\right], \tag{4.4}$$

$$\mathbf{e}\times\mathbf{n} = \frac{a}{b}\mathbf{i}_1 + \sin\left(\frac{x}{b}\right)\mathbf{i}_2 - \cos\left(\frac{x}{b}\right)\mathbf{i}_3, \tag{4.5}$$

$$\tau\mathbf{n} = -\frac{\partial(\mathbf{e}\times\mathbf{n})}{\partial l} = -\frac{1}{b}\left[\cos\left(\frac{x}{b}\right)\mathbf{i}_2 + \sin\left(\frac{x}{b}\right)\mathbf{i}_3\right]. \tag{4.6}$$

Therefrom, the curvature of the asymptotic helix is

$$\kappa = \frac{a}{b^2} \tag{4.7}$$

and the torsion is

$$\tau = \frac{1}{b}. \tag{4.8}$$

In these terms, relation (4.2) looks as

$$\kappa \ll \tau. \tag{4.9}$$

It is implicit here that the direction of the filament's vorticity coincides with the vector **e**. Hence, the motion of the filament can be calculated using (2.6). Substituting (4.5) with (4.7), (4.8) into (2.6), and neglecting the small velocity component along the x-axis, we get

$$\mathbf{u} = a\nu\tau^2\left[\sin(\tau x)\mathbf{i}_2 - \cos(\tau x)\mathbf{i}_3\right]. \tag{4.10}$$

So, the helix rotates counterclockwise around the x-axis (looking in the direction of the x-axis) with the constant angular velocity

$$\omega = \nu\tau^2. \tag{4.11}$$

Taking into account the angular displacement, the initial relation (4.1) should be improved

$$y = a\cos(\tau x - \nu\tau^2 t), \qquad z = a\sin(\tau x - \nu\tau^2 t). \tag{4.12}$$

This provides the solution to the basic equation (3.7).

5. Schrödinger equation

From the above we see that when $a\tau \ll 1$, the motion of the vortex filament reduces itself to a plane vector mechanics. By virtue of this, relations (4.12) can be represented as a complex function $\varphi(x,t)$ of real variables

$$\begin{aligned}\varphi(x,t) &= a\left[\cos(\tau x - \nu\tau^2 t) + i\sin(\tau x - \nu\tau^2 t)\right] \\ &= a\exp\left[i(\tau x - \nu\tau^2 t)\right].\end{aligned} \tag{5.1}$$

In this connection, the vector form (3.6), $\mathbf{i}_1 \times (y\mathbf{i}_2 + z\mathbf{i}_3) = -z\mathbf{i}_2 + y\mathbf{i}_3$, which (3.7) is based on, corresponds to the relation for complex values

$$i(y + iz) = -z + iy. \tag{5.2}$$

This puts (3.7) into the form of the Schrödinger equation

$$\frac{\partial\varphi}{\partial t} = i\nu\frac{\partial^2\varphi}{\partial x^2}, \tag{5.3}$$

where

$$\varphi = y(x,t) + iz(x,t). \tag{5.4}$$

Equation (5.3), or (3.7), has a simple geometrical meaning. In a helix, the principal normal $\mathbf{n}$ lies in a plane, which is perpendicular to the x-axis, and it is directed to the x-axis (see (4.4)). When $a\tau \ll 1$, the tangent $\mathbf{e}$ is almost parallel to the x-axis. So, in order to get from it the self-induction velocity (2.6), we must merely rotate $\mathbf{n}$ at the angle $\pi/2$ counterclockwise around the x-axis if looking against this axis. In terms of complex values, the curvature

$$\kappa n = \frac{\partial^2\varphi}{\partial x^2}. \tag{5.5}$$

The operation $i\kappa n$ corresponds to the above-mentioned rotation of n. The self-induction velocity is

$$u = \frac{\partial \varphi}{\partial t}. \tag{5.6}$$

Here φ, n, and u are complex values and x, t, κ are real values.

6. The wave packet

So, the above-discussed asymptotic solution can be represented in the form of the hypercomplex value r:

$$r(x,t) = i_1 x + \varphi(x,t), \tag{6.1}$$

where x, t are real values. According to the above, the complex-valued function $\varphi(x,t)$ can be expanded into the sum of harmonics

$$\varphi(x,t) = \int c(\tau) \exp\left[i(\tau x - \nu\tau^2 t)\right] d\tau. \tag{6.2}$$

As usual, taking this integral in the range $[\tau_0 - \Delta\tau, \tau_0 + \Delta\tau]$, we get the wave packet

$$a\frac{\sin\left[(x - 2\nu\tau_0)\Delta\tau\right]}{(x - 2\nu\tau_0)\Delta\tau} \exp\left[i(\tau_0 x - \nu{\tau_0}^2 t)\right] \tag{6.3}$$

(see Figure 6.1). The hump of the wave packet moves translationally with the velocity

$$\upsilon = 2\nu\tau_0. \tag{6.4}$$

The remarkable feature of this phenomenon is that the motion of the hump is due to the rotation of an individual helix with the angular velocity $\nu\tau^2$ but not because of its longitudinal motion. This is the effect of a screw! A bolt is screwed into a nut due to rotation. In general, the velocity υ of screwing in depends on the thread b as ωb. From (4.11), (4.8), we have for the vortex helix $\omega \sim 1/b^2$. Therefore, $\upsilon \sim 1/b$, that is in accord with (6.4).

As we will see in the next section the wave packet gives us an approximation for the asymptotic solution to the nonlinear equation (2.7) constructed from the solutions to the corresponding linear equation (3.7).

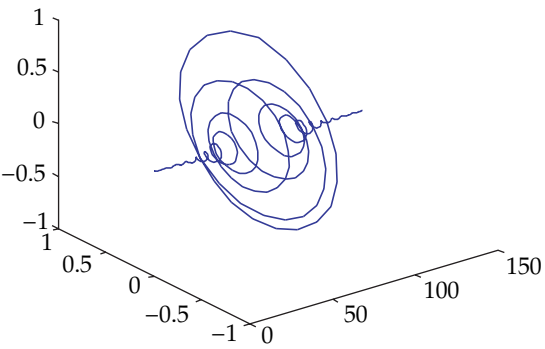

FIGURE 6.1. A wave packet (6.3).

7. Soliton

Equation (2.7) possesses the following exact solution $\mathbf{r}(l,t)$ (see [5]):

$$\begin{gathered}\mathbf{r} = x\mathbf{i}_1 + y\mathbf{i}_2 + z\mathbf{i}_3, \quad x = l - a\tanh\eta, \\ y + iz = a\operatorname{sech}\eta\exp(i\theta),\end{gathered} \tag{7.1}$$

where

$$a = \frac{2\hat{\kappa}}{\hat{\kappa}^2 + \tau^2}, \tag{7.2}$$

$$\eta = \hat{\kappa}(l - 2\nu\tau t), \tag{7.3}$$

$$\theta = \tau l + \nu\left(\hat{\kappa}^2 - \tau^2\right)t, \quad \tau = \text{const}, \ \hat{\kappa} = \text{const}. \tag{7.4}$$

As before, ν is the self-induction coefficient of the vortex filament.

In order to form the curvilinear configuration on the straight line, we need an extra segment of the filament, which will be further referred to as the redundant segment. Its length is easily found integrating the differential of (7.1) all over the x-axis

$$\int dx = \int dl - a\int d\tanh\eta \tag{7.5}$$

whence

$$[l - x]_{-\infty}^{+\infty} = 2a. \tag{7.6}$$

Substituting $\mathbf{r}(l,t)$ into (2.3) we find that the curvature of the line is described by the bell-shaped function

$$\kappa(l,t) = 2\hat{\kappa}\operatorname{sech}\eta. \tag{7.7}$$

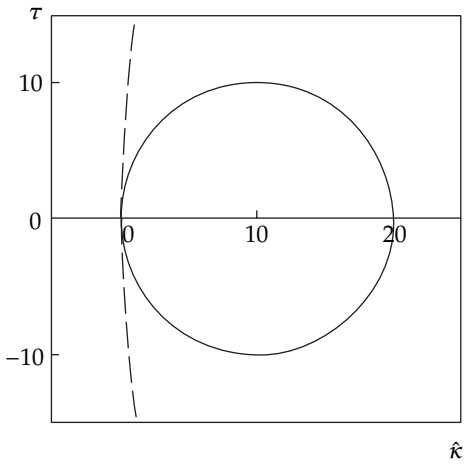

FIGURE 7.1. The torsion τ in relation to curvature parameter $\hat{\kappa}$ plotted by (7.2) with a = const. Solid line: $a = 0.1$; dashed line: $a = 0.01$.

Its parameter $l/\hat{\kappa}$ from (7.3) can be used as a measure of the disturbance's delocalization. So, the more the line is curved, the more the inclusion of the redundant segment (7.6) is localized.

Substituting $\mathbf{r}(l,t)$ into (2.4), we find that the parameter τ has the meaning of the curve's torsion.

According to (7.3), the soliton moves steadily along the vortex filament with the velocity

$$v = 2\nu\tau. \tag{7.8}$$

The curve rotates around the x-axis with the angular velocity

$$\omega = \frac{\partial(y+iz)/\partial t}{\left(y^2+z^2\right)^{1/2}}. \tag{7.9}$$

We may rewrite (7.2) in a more convenient form

$$\left(\hat{\kappa} - \frac{1}{a}\right)^2 + \tau^2 = \frac{1}{a^2}. \tag{7.10}$$

Now, assuming that a is constant, it is easily seen (Figure 7.1) how the longitudinal extension of the disturbance, measured by $1/\hat{\kappa}$, affects the curve's torsion and the corollaries.

When the disturbance is most localized, that is, the curvature is maximal $\hat{\kappa} = 2/a$, then $\tau = 0$ (Figure 7.1). That is, the curve is plane. It has the form of a loop. In accord with (7.8) the plane loop is translationally

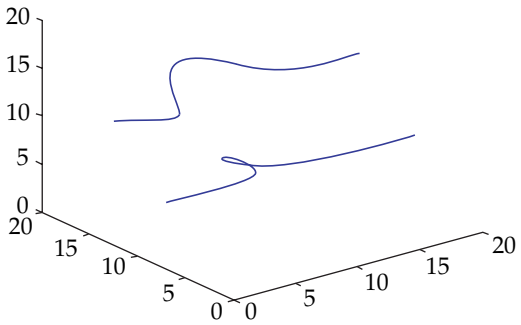

FIGURE 7.2. The loop-shaped soliton on a vortex filament at $\tau/\hat{\kappa} = 0.23$ (bottom) and $\tau/\hat{\kappa} = 1.1$ (top).

at rest. It rotates steadily around the x-axis with the angular velocity $\omega = \nu\hat{\kappa}^2$.

As the disturbance's spread increases from $a/2$ to a, that is, as the curvature decreases to $\hat{\kappa} = 1/a$, the torsion τ grows to its maximal value $1/a$ (Figure 7.1). It corresponds to maximal value of the soliton's translational velocity (7.8)

$$v \le \frac{2\nu}{a}. \tag{7.11}$$

In this range of the delocalization

$$\frac{\tau}{\hat{\kappa}} < 1. \tag{7.12}$$

The filament is convolved into a loop (Figure 7.2, bottom) and the direction of its rotation coincides with that of the vorticity of the unperturbed filament.

Further, as the disturbance delocalizes from a to ∞, the torsion drops from $1/a$ to zero (Figure 7.1). In this range,

$$\frac{\tau}{\hat{\kappa}} > 1. \tag{7.13}$$

The loop is unfolded (Figure 7.2, top), and thus, the rotation becomes opposite to the vorticity.

When $\hat{\kappa} \to 0$, we have $\tau \to 0$. In this event,

$$\hat{\kappa} \ll \tau \tag{7.14}$$

and, in accord with (4.9), the curve tends to an asymptotic helix. This is the humped helix approximated by the wave packet (6.3). The asymptotic helix rotates steadily around the x-axis with angular velocity (4.11) $\omega = \nu\tau^2$.

Differentiating (2.7) with respect to l and using formula (2.1), we get a positionally invariant form of the motion law

$$\frac{\partial \mathbf{e}}{\partial t} = \nu \mathbf{e} \times \frac{\partial^2 \mathbf{e}}{\partial l^2}. \tag{7.15}$$

It was shown rigorously [5] that, with (2.3), (2.4), this equation can be transformed to the nonlinear Schrödinger equation

$$-\frac{i}{\nu}\frac{\partial \Phi}{\partial t} = \frac{\partial^2 \Phi}{\partial l^2} + \frac{1}{2}|\Phi|^2\Phi \tag{7.16}$$

under the substitution

$$\Phi = \kappa \exp\left[i\left(\int_0^l \tau\, dl - \omega t\right)\right], \tag{7.17}$$

where $\omega = \text{const}$ is the energy integral of motion.

When

$$\kappa \ll \tau, \tag{7.18}$$

the second term in the right-hand side of (7.16) can be neglected and the equation linearized to (5.3). In this event

$$\Phi \longrightarrow \varphi = \kappa \exp\left\lfloor i(\tau x - \nu\tau^2 t)\right\rfloor, \tag{7.19}$$

where $\kappa \to a\tau^2$. So, the wave function takes the meaning of the helix rotation velocity (4.10).

8. Integrals of motion

With (7.17), (7.16) can be presented in the quasihydrodynamic form

$$\frac{\partial \rho}{\partial t} + \frac{\partial(\rho v)}{\partial l} = 0, \tag{8.1}$$

$$\frac{\partial(\rho v)}{\partial t} + \frac{\partial}{\partial l}\left[\rho v^2 - \nu^2 \rho \frac{\partial^2 \ln \rho}{\partial l^2} - \frac{1}{2}\nu^2\rho^2\right] = 0, \tag{8.2}$$

where

$$\rho = \kappa^2 = |\Phi|^2, \tag{8.3}$$

$$\upsilon = 2\nu\tau. \tag{8.4}$$

Through (2.6), the part ε of the kinetic energy of the fluid due to distortion of the vortex filament is given by

$$\varepsilon = \frac{1}{2}\varsigma \int u^2\, dl = \frac{1}{2}\varsigma\nu^2 \int \kappa^2\, dl = \frac{1}{2}\varsigma\nu^2 \int \rho\, dl, \tag{8.5}$$

where ς stands for linear density of the fluid along the filament and (8.3) was used. The energy ε has the meaning of the self-energy of the disturbance and can be interpreted as the mass m_ε of this disturbance. By virtue of the continuity equation (8.1), this quantity is conserved as follows:

$$\frac{\partial}{\partial t}\int \rho\, dl = 0. \tag{8.6}$$

Thus, the density of the distribution of the distortion energy along the vortex filament corresponds to the linear density of the space distribution of the soliton's mass m_ε

$$m_\varepsilon \frac{\varsigma u^2/2}{\varepsilon} = m_\varepsilon \frac{\varsigma\nu^2\rho/2}{\varepsilon}. \tag{8.7}$$

In these terms, the flow of the distortion energy along the filament

$$\frac{1}{2}\varsigma\nu^2\rho\upsilon \tag{8.8}$$

acquires the meaning of the soliton's local momentum. From the dynamic equation (8.2), we see that the total momentum of the soliton is conserved as follows:

$$\frac{\partial}{\partial t}\int \rho\upsilon\, dl = 0. \tag{8.9}$$

Next, using (8.7), the soliton's translational energy can be considered

$$E_t = \frac{1}{2}\int m_\varepsilon \frac{\varsigma\nu^2\rho/2}{\varepsilon}\upsilon^2\, dl. \tag{8.10}$$

The contribution of the diffusion flow

$$\rho w = -\nu \frac{\partial \rho}{\partial l} \tag{8.11}$$

should be also taken into account. In the nonlinear case, we must include in the integral the term from (8.2) of the binding energy

$$-\frac{1}{2}\nu^2\rho^2. \tag{8.12}$$

Then, the total energy is conserved as

$$\frac{\partial}{\partial t}\int \frac{1}{2}\rho\left(v^2 + w^2 - \nu^2\rho\right) dl = 0. \tag{8.13}$$

We may also add the density of the external force to the dynamic equation (8.2). For the potential force, it looks as

$$\frac{\partial(\rho v)}{\partial t} + \frac{\partial}{\partial l}\left[\rho v^2 - \nu^2\rho\frac{\partial^2 \ln\rho}{\partial l^2} - \frac{1}{2}\nu^2\rho^2\right] + \rho\frac{\partial U}{\partial l} = 0. \tag{8.14}$$

When the potential $U(l)$ does not depend on the time, the following quantity is conserved:

$$\int \rho\left[\frac{1}{2}\left(v^2 + w^2 - \nu^2\rho\right) + U\right] dl. \tag{8.15}$$

Thence, the nonlinear Schrödinger equation with the potential energy U should be written as

$$-\frac{i}{\nu}\frac{\partial\Phi}{\partial t} = \frac{\partial^2\Phi}{\partial l^2} + \frac{1}{2}|\Phi|^2\Phi - \frac{1}{\nu^2}U\Phi. \tag{8.16}$$

Substituting (7.7) to the second integral in (8.5), we get the soliton's self-energy

$$\varepsilon = 4\varsigma\nu^2\hat{\kappa}. \tag{8.17}$$

The soliton's translational energy E_t is easily found if we will substitute (8.4) with $\tau = \text{const}$ into (8.10)

$$E_t = m_\varepsilon \frac{2\nu^2\tau^2}{\varepsilon}\frac{1}{2}\varsigma\nu^2\int \rho\, dl. \tag{8.18}$$

Then, using in this expression (8.5), we get

$$E_t = 2m_\varepsilon v^2 \tau^2. \tag{8.19}$$

In asymptotics, when $\hat{\kappa}/\tau \to 0$, relation (7.2) reduces itself to

$$2\hat{\kappa} = a\tau^2. \tag{8.20}$$

Then, we have for (8.17)

$$\varepsilon = 2\varsigma v^2 a\tau^2. \tag{8.21}$$

We see that expression (8.21) for the fluid energy coincides with that (8.19) for the soliton's kinetic energy if we take for the mass of the asymptotic soliton

$$m_\varepsilon = \varsigma a. \tag{8.22}$$

This enables us to identify the energy integral of motion of the asymptotic soliton with the real energy of the fluid motion, and the mass of the soliton—with the real mass (8.22) of the fluid.

9. Particle

In this section, we demonstrate with a simplified model that there exists a singular unique size of the loop-shaped soliton on a vortex filament. The redundant segment (7.6) of the filament, needed in order to form the curvilinear configuration on the originally straight line, brings with itself the energy of the fluid motion

$$2a\xi, \tag{9.1}$$

where ξ is the energy density on a unit length of the filament. The energy of distortion associated with the loop is given by (8.17). For the plane configuration of the loop, it equals

$$\varepsilon = \frac{8\varsigma v^2}{a}, \tag{9.2}$$

where (7.2) with $\tau = 0$ was used. Summing (9.1) and (9.2), we find the total energy of the fluid associated with the loop as a function of the redundant length $2a$

$$2a\xi + \frac{8\varsigma v^2}{a}. \tag{9.3}$$

This function has a minimum at

$$a = 2\nu\left(\frac{\varsigma}{\xi}\right)^{1/2} \tag{9.4}$$

which determines the singular size of the loop. The same is valid with respect to the vortex ring obtained from the loop by reconnection of the filament at the point of intersection.

For visuality, we reproduce the whole argumentation for the vortex ring. The fluid energy associated with the length is evaluated by

$$2\pi R\xi, \tag{9.5}$$

where R is the radius of the ring. Its curvature is given by

$$\kappa = \frac{1}{R}. \tag{9.6}$$

So, the energy of distortion associated with the ring is found from the integral in (8.5) as

$$\varepsilon = \frac{1}{2}\varsigma\nu^2\left(\frac{1}{R}\right)^2 2\pi R. \tag{9.7}$$

Then, the total energy is given by

$$2\pi\xi R + \frac{\pi\varsigma\nu^2}{R}. \tag{9.8}$$

Comparing it with (9.3), we see that a has the meaning of the loop's diameter.

The filament is taken in the current model as the idealization of the vortex tube. In the perfect fluid, the vortex tube is hollow inside. So, the curvilinear configuration of the tube—the helix, the loop, or the vortex ring—just corresponds to the inclusion of a redundant void in the discrete structure of the vortex sponge. This agrees well with the mesoscopic mechanical model of a particle [3, 4]. Although, the mass $\varsigma 2a$ of the redundant segment (7.6) of the vortex tube appears to be twice the mass of the disturbance that is computed using formula (8.22) for asymptotic helix.

It is clear that the construction described ensures the discreteness of a nonlinear configuration in the structure of the vortex sponge, provided that the strength of the vortex tube is fixed.

A plane loop on a vortex filament cannot be split into smaller plane loops without the input of some fluid energy. Indeed, let it be divided

into two parts α and $1-\alpha$, where $1>\alpha>0$. As seen from (9.1), (7.6), the energy of the background is additive, and thus, does not change in splitting. Whereas the energy of disturbance computed with (9.2) increases as follows:

$$\frac{1}{\alpha}+\frac{1}{1-\alpha}>1. \tag{9.9}$$

However, the plane loop can be split into nonplanar solitons, that is, into waves. This process needs some increase in the secondary integral of energy (8.10). Thus, we have from (7.2) that the plane loop with the curvature κ (7.7) can be split into m waves with the curvature κ/m and for $m\gg 1$ with the torsion $\tau\approx\hat{\kappa}$. According to (7.8), a nonplanar soliton moves translationally with the velocity $2\nu\tau$. Requiring the conservation (8.9) of the momentum, we find that the splinters move in opposite directions.

In asymptotics, when $\kappa/\tau\to 0$, we have (8.21) instead of (9.2). Now, the distortion energy is additive with respect to division of the redundant segment (7.6). So, the helix can be split as a classical mass body.

10. Elementary helix

As we see in (7.11), the velocity of the given soliton is restricted from above by

$$v_{\max}=\frac{2\nu}{a} \tag{10.1}$$

(see Figure 7.1). In its turn, $v_{\max}$ is restricted by some fundamental constant c, which must be the speed of the perturbation wave in the turbulent medium:

$$v_{\max}\le c. \tag{10.2}$$

This implies that

$$a\ge\frac{2\nu}{c}. \tag{10.3}$$

Thus, we come to the concept of the elementary inclusion, having the minimal size of the redundant segment

$$a_0=\frac{2\nu}{c}. \tag{10.4}$$

It probably exists only as an asymptotic helix. In this model c corresponds [7] to the speed of light in vacuum.

On the other side, condition (7.14) of the asymptotic case can be written as

$$\frac{2\hat{\kappa}}{\tau} \leq \beta \ll 1, \tag{10.5}$$

where β is an upper bound for the asymptoticity. Combining it with (8.20), (7.8) gives

$$\upsilon \leq \frac{2\nu}{a}\beta. \tag{10.6}$$

This shows that the domain of velocities for which the linear Schrödinger equation is valid broadens with the decrease in the length of the redundant segment (Figure 7.1, the left side).

So, in order to increase the maximal velocity of the disturbance, we must divide the inclusion of the redundant segment $2a$ into parts.

11. Thermalization

Supposedly, under the action of the stochastic medium, the soliton on a vortex filament splits into the elementary helices mentioned above.

We see the thermalized soliton as a system of m identical segments $a_0 = a/m$ each of which obeys the linear Schrödinger equation (5.3). For this system, a single many-body equation can be formally composed

$$\frac{\partial \Psi}{\partial t} = i\nu \sum_{n=1}^{m} \frac{\partial^2 \Psi}{\partial x_n^2}, \tag{11.1}$$

where the function Ψ is given by the product of the forms (7.19)

$$\Psi = \prod_{n=1}^{m} \kappa_n \exp\left[i\left(\tau_n x_n - \nu \tau_n^2 t\right)\right]. \tag{11.2}$$

Passing in (11.1) to the center point variable

$$x = \frac{1}{m}\sum_{n=1}^{m} x_n, \tag{11.3}$$

we may get, via the well-known procedure, the equation

$$\frac{\partial \psi}{\partial t} = i\frac{\nu}{m}\frac{\partial^2 \psi}{\partial x^2}. \tag{11.4}$$

This rather formal result can be visualized if we consider the phase of the wave function (11.2), which is taken for m helices with equal values $\tau_n = \tau$ of the torsion

$$\sum_{n=1}^{m} (\tau_n x_n - \nu\tau_n^2 t) \longrightarrow \tau \sum_{n=1}^{m} x_n - m\nu\tau^2 t = (m\tau)x - \frac{\nu}{m}(m\tau)^2 t = kx - \frac{\nu}{m}k^2 t, \tag{11.5}$$

where

$$k = m\tau \tag{11.6}$$

and x is given by (11.3).

Provided that the length $2a_0$ of an elementary segment is constant, the number m of elementary constituents involved in the soliton can be taken as a measure of the soliton's mass, the real mass being

$$m_\varepsilon = \varsigma a = m\varsigma a_0, \tag{11.7}$$

where (8.22) was used. Then, the quantity k defined above in (11.6) can be taken as a measure of the soliton's momentum

$$p = \varsigma a v = \varsigma a_0 2\nu m\tau = 2\nu\varsigma a_0 k, \tag{11.8}$$

where (8.4) was used. The frequency term in the phase (11.5) of the wave function acquires the meaning of the soliton's kinetic energy (8.19)

$$E = \frac{p^2}{2m\varsigma a_0} = 2\nu\varsigma a_0 \frac{\nu k^2}{m}. \tag{11.9}$$

In quantum mechanics, the constant analogous to ν is usually designated as

$$\nu\varsigma a_0 = \frac{\hbar}{2}. \tag{11.10}$$

12. Collapse

A fluctuation of the fluid pressure may cause the spatial distribution of splinters to re-collect into the original soliton. We describe this process phenomenologically adding to (11.1) the pairwise attraction between the elementary helices

$$\frac{\partial \Psi}{\partial t} = i\nu \left(\sum_{n=1}^{m} \frac{\partial^2 \Psi}{\partial x_n^2} - \frac{1}{\nu^2} U\Psi \right), \tag{12.1}$$

where the mass density of the potential is given by

$$U = -\frac{4\nu^2\hat{\kappa}}{m}\sum_{s<q}^{m}\delta(x_s - x_q). \tag{12.2}$$

In (12.1), the potential was introduced in the same way as it was done in (8.16). In (12.2), the coefficient before the δ-function was chosen in accord with (8.17) assuming that the self-energy of the fragment is $1/m$ of the self-energy (8.17) of the original soliton.

Equation (12.1) with (12.2) can be solved exactly. However, it is illuminating to give the scheme based on Hartree approximation

$$\Psi = \prod_{n=1}^{m}\varphi_n(x_n,t), \tag{12.3}$$

where φ_n is the wave function of a splinter

$$\frac{\partial\varphi_n}{\partial t} = i\nu\frac{\partial^2\varphi_n}{\partial x_n^2}. \tag{12.4}$$

Compare (12.3) with (11.2). By (8.5), (8.3), the self-energy of the splinter is computed via

$$\frac{1}{2}\varsigma\nu^2\int|\varphi_n|^2\,dx_n. \tag{12.5}$$

This energy was taken in (12.2) to be $1/m$ of the self-energy (8.17) of the original soliton

$$\frac{4\varsigma\nu^2\hat{\kappa}}{m}. \tag{12.6}$$

That implies the following normalization of φ_n:

$$\int|\varphi_n|^2\,dx_n = \frac{8\hat{\kappa}}{m}, \quad n = 1,2,\ldots,m. \tag{12.7}$$

Substituting (12.3) into (12.1) with (12.2) and multiplying it by

$$\prod_{n=2}^{m}\varphi_n^*(x_n,t)\,dx_n \tag{12.8}$$

and then integrating over all x_n, where $n \neq 1$, we get

$$-\frac{i}{\nu}\frac{\partial\varphi}{\partial t} = \frac{\partial^2\varphi}{\partial x^2} + \frac{1}{2}(m-1)|\varphi|^2\varphi + \frac{m(m-1)(m-2)}{32\hat{\kappa}}\varphi\int|\varphi|^4\,dx. \tag{12.9}$$

Taking

$$\phi = (m-1)^{1/2}\varphi\exp\left(-i\omega_0 t\right), \tag{12.10}$$

where

$$\omega_0 = \nu\frac{m(m-1)(m-2)}{32\hat{\kappa}}\int|\varphi|^4\,dx, \tag{12.11}$$

we come to

$$-\frac{i}{\nu}\frac{\partial\phi}{\partial t} = \frac{\partial^2\phi}{\partial x^2} + \frac{1}{2}|\phi|^2\phi. \tag{12.12}$$

This equation coincides with (7.16) when $l \to x$, that is, when $\kappa \ll \tau$. Note that for $m \gg 1$ (12.10) with (12.7) gives the following normalization of the wave function ϕ:

$$\frac{1}{2}\int|\phi|^2\,dx = 4\hat{\kappa}. \tag{12.13}$$

Compare (12.13) with (8.17) obtained from (8.5), (8.3) with (7.7)

$$\varepsilon = \frac{1}{2}\varsigma\nu^2\int|\Phi|^2\,dl = 4\varsigma\nu^2\hat{\kappa}. \tag{12.14}$$

So, the quantum definition of the particle's mass, given in Section 11, agrees with its mechanical definition given in Section 8.

Similar results can be obtained in a simpler model if we take in (12.2) $s = 1$, $q = 2,\ldots,m$.

The choice of the place or splinter, where the soliton will be recollected, is the competence of a more general model of the measurement, in which the above scheme should be included. We may expect that it is probabilistic and the probability density is proportional to local decrease in the fluid pressure. By hydrodynamics [3], the decrement of the pressure equals to the increase in the energy density, that is, it is proportional to $|\varphi|^2$ from (11.4) or a similar equation.

13. Spin

There are two kinds of helix which differ in the sign of the torsion τ. The right-hand screw helix (Figure 4.1, bottom) is described by (4.1)

$$y = a\cos(\tau x), \qquad z = a\sin(\tau x) \tag{13.1}$$

with $\tau > 0$. The left-hand screw (Figure 4.1, top) is described by (13.1) with $\tau < 0$. According to (4.10), the helix rotates around the x-axis with the velocity

$$\mathbf{u} = av\tau^2\left[\sin(\tau x)\mathbf{i}_2 - \cos(\tau x)\mathbf{i}_3\right]. \tag{13.2}$$

As we see from this, both kinds rotate in the same direction—counter to the direction of the filament's vorticity, which was chosen in (13.2) so as to coincide with the direction of the x-axis.

According to (7.8), or (6.4), the helix moves translationally with the velocity

$$v = 2v\tau. \tag{13.3}$$

That is, the right-hand screw helix travels in the direction which the filament's vorticity points to. The left-hand screw helix goes in the opposite direction.

In three dimensions, we deal with the ideal fluid pierced in all directions by the vortex filaments [6]. Macroscopically (to be more precise, mesoscopically), this system looks like a turbulent ideal fluid. Perturbations of the turbulence was shown [7] to reproduce a system of the form of the electromagnetic fields. In particular, the average fluid velocity $\langle\mathbf{u}\rangle$ corresponds to the magnetic vector-potential. The rotation of the soliton is seen macroscopically as a singularity—the center of torsion in the quasielastic medium. It corresponds to a magnetic dipole $\boldsymbol{\mu}$. The energy of its interaction with the external vorticity field is given by

$$-\boldsymbol{\mu}\cdot\mathrm{curl}\langle\mathbf{u}\rangle. \tag{13.4}$$

The fluid vorticity $\mathrm{curl}\langle\mathbf{u}\rangle$ just corresponds to the magnetic field.

Let two kinds of the helices move in the turbulent substratum from the left to the right. The first helix (Figure 13.1, bottom) is a right-hand screw; hence, it moves along a filament whose vorticity is also directed to the right. The other helix (Figure 13.1, top) is the left-hand screw. So,

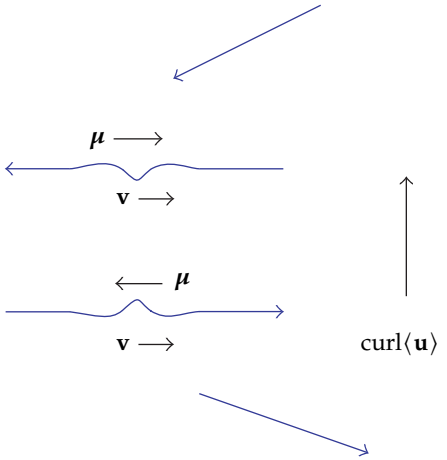

FIGURE 13.1. A right-hand screw helix (bottom) and left-hand screw helix (top) traveling from the left to the right in the vortex sponge through an inhomogeneous field of fluid vorticity curl$\langle \mathbf{u} \rangle$. Arrows on the filaments indicate the direction of their vorticity, $\mathbf{v}$ shows the direction of the translational motion and $\boldsymbol{\mu}$ the rotational moment of the helices.

it moves to the right along a filament whose vorticity is directed opposite to the direction of the motion. The question is how an observer may distinguish between these two cases.

A discrimination can be done imposing on them an external field of fluid vorticity curl$\langle \mathbf{u} \rangle$. So, we have the conditions of the Stern-Gerlach experiment. The vertical arrow at Figure 13.1 just shows the fluid vorticity directed and growing from the bottom to the top. This inhomogeneous vorticity field will deflect the traveling helices so as to diminish their energy in accord with formula (13.4). In order to change somewhat the direction of its motion, a helix must jump over to the adjacent filament with similar but slightly different direction of vorticity. Thus, the helices will act in the same way (see Figure 13.1) as spin particles in the real Stern-Gerlach experiment.

14. Conclusion

The above-constructed mechanical model reproduces the main features of a microparticle including its discreteness. However, there is a point that should be still elucidated. This is the discrete structure of the vortex sponge, that is, the fixed strength of the intrinsic vortex tube, or filament. For the time being, it is taken as a postulate.

References

[1] G. K. Batchelor, *An Introduction to Fluid Dynamics*, Cambridge University Press, Cambridge, 1970.

[2] V. P. Dmitriyev, *Particles and charges in the vortex sponge*, Z. Naturforsch **48a** (1993), no. 8-9, 935–942.

[3] ———, *Towards an exact mechanical analogy of particles and fields*, Nuovo Cimento **111A** (1998), no. 5, 501–511.

[4] ———, *Mechanical analogies for the Lorentz gauge, particles and antiparticles*, Apeiron **7** (2000), no. 3-4, 173–183.

[5] H. Hasimoto, *A soliton on a vortex filament*, J. Fluid Mech. **51** (1972), 477–485.

[6] E. M. Kelly, *Vacuum electromagnetics derived exclusively from the properties of an ideal fluid*, Nuovo Cimento **32B** (1976), no. 1, 117–137.

[7] O. V. Troshkin, *On wave properties of an incompressible turbulent fluid*, Physica A **168** (1990), no. 2, 881–899.

Valery P. Dmitriyev: Lomonosov University, P.O. Box 160, Moscow 117574, Russia

E-mail address: dmitr@cc.nifhi.ac.ru

Journal of Applied Mathematics and Decision Sciences

Special Issue on Decision Support for Intermodal Transport

Call for Papers

Intermodal transport refers to the movement of goods in a single loading unit which uses successive various modes of transport (road, rail, water) without handling the goods during mode transfers. Intermodal transport has become an important policy issue, mainly because it is considered to be one of the means to lower the congestion caused by single-mode road transport and to be more environmentally friendly than the single-mode road transport. Both considerations have been followed by an increase in attention toward intermodal freight transportation research.

Various intermodal freight transport decision problems are in demand of mathematical models of supporting them. As the intermodal transport system is more complex than a single-mode system, this fact offers interesting and challenging opportunities to modelers in applied mathematics. This special issue aims to fill in some gaps in the research agenda of decision-making in intermodal transport.

The mathematical models may be of the optimization type or of the evaluation type to gain an insight in intermodal operations. The mathematical models aim to support decisions on the strategic, tactical, and operational levels. The decision-makers belong to the various players in the intermodal transport world, namely, drayage operators, terminal operators, network operators, or intermodal operators.

Topics of relevance to this type of decision-making both in time horizon as in terms of operators are:

- Intermodal terminal design
- Infrastructure network configuration
- Location of terminals
- Cooperation between drayage companies
- Allocation of shippers/receivers to a terminal
- Pricing strategies
- Capacity levels of equipment and labour
- Operational routines and lay-out structure
- Redistribution of load units, railcars, barges, and so forth
- Scheduling of trips or jobs
- Allocation of capacity to jobs
- Loading orders
- Selection of routing and service

Before submission authors should carefully read over the journal's Author Guidelines, which are located at http://www.hindawi.com/journals/jamds/guidelines.html. Prospective authors should submit an electronic copy of their complete manuscript through the journal Manuscript Tracking System at http://mts.hindawi.com/, according to the following timetable:

Manuscript Due	June 1, 2009
First Round of Reviews	September 1, 2009
Publication Date	December 1, 2009

Lead Guest Editor

Gerrit K. Janssens, Transportation Research Institute (IMOB), Hasselt University, Agoralaan, Building D, 3590 Diepenbeek (Hasselt), Belgium; Gerrit.Janssens@uhasselt.be

Guest Editor

Cathy Macharis, Department of Mathematics, Operational Research, Statistics and Information for Systems (MOSI), Transport and Logistics Research Group, Management School, Vrije Universiteit Brussel, Pleinlaan 2, 1050 Brussel, Belgium; Cathy.Macharis@vub.ac.be